Biochimica et Biophysica Acta, 1015 (1990) 471–481
Elsevier

BBABIO 43150

Photosynthetic electron transfer in *Heliobacterium chlorum* studied by EPR spectroscopy

Monika R. Fischer

Department of Biophysics, Huygens Laboratory of the State University, Leiden (The Netherlands)

(Received 16 May 1989)
(Revised manuscript received 5 September 1989)

Key words: Electron transfer; Acceptor; Triplet; Photosynthesis; EPR; (*H. chlorum*)

The photosynthetic electron transfer chain of *Heliobacterium chlorum* has been studied by low-temperature EPR under different redox conditions. The EPR signal of the oxidized primary donor P-798$^+$ was a near-gaussian, with width $\Delta B = 1.05$ mT, corroborating the result of Prince et al. (Prince, R.C., Gest, H. and Blankenship, R.E. (1985) Biochim. Biophys. Acta 810, 377–384). Under reducing conditions a complex behaviour in the $g = 2.00$ region was found, which is interpreted as being due to at least two acceptors besides the iron-sulphur cluster. Simulations with a bacteriochlorophyll and a quinone as acceptors agree well with the experimental results, when it was assumed that they are both partially reduced, either because of reaction centre heterogeneity or because of frozen-in charge distribution over the two acceptors. In addition to these $g = 2.00$ acceptor signals a triplet signal is present, composed of an antenna- and a reaction centre triplet with zero-field splitting parameters $|D| = 240 \cdot 10^{-4}$ and $226 \cdot 10^{-4}$ ($\pm 10 \cdot 10^{-4}$) cm^{-1}, and $|E| = 88 \cdot 10^{-4}$ and $74 \cdot 10^{-4}$ ($\pm 10 \cdot 10^{-4}$) cm^{-1}, respectively. Furthermore a split-line signal was found, which is very similar to that found in Photosystem II (Rutherford, A.W. and Thurnauer, M.C. (1982) Proc. Natl. Acad. Sci. USA 79, 7283–7287), attributed to a magnetic interaction between a secondary donor and one of the $g = 2.00$ acceptors.

Introduction

The strictly anaerobic photosynthetic bacterium, *Heliobacterium chlorum,* has been known for only a few years [1,2]. *H. chlorum* is not specifically related to any of the four groups of photosynthetic prokaryotes [3]. Phylogenetically seen, however, it is most related to the Gram-positive group of bacteria [4]. Until now the Heliobacteria are the only photosynthetic organisms known to belong to this group. *H. chlorum* contains the previously unknown bacteriochlorophyll (BChl) *g*, and although there are differences in the photosynthetic apparatus, there are some properties similar to those of other groups. On the one hand some optical [5,6] and thermodynamical [7] properties indicate a relationship with the photosystem of the green sulphur bacteria, but *H. chlorum* does not have the chlorosomes characteristic for these bacteria. On the other hand, the structure of BChl *g* (a vinyl instead of the acetyl group on ring I) and the absorbance difference spectrum seem to link the photosystem of *H. chlorum* to that of Photosystem I [8–10]. Comparison of the different photosynthetic species could yield more information on the evolutionary course. Examination of the properties of *H. chlorum*, especially of its electron transfer mechanism, is therefore of great interest.

Optical measurements show that a membrane-bound *c*-type cytochrome is involved in light-induced electron transport, as also found in the green bacterium *Chloroflexus aurantiacus* [8]; at 5 K this cytochrome is unable to donate electrons to the reaction centre [7]. The primary electron donor P-798 consists of BChl *g*; optical measurements [10] suggest that it is a monomer, whereas EPR measurements are ambiguous [7,11]. Subtraction of the absorbance difference spectra at 150 ps and at 1.5 ns after a saturating laser flash yields a spectrum very similar to that observed for the inter-

Abbreviations: A_0, first electron acceptor; A_1, second electron acceptor; ADMR, absorbance-detected magnetic resonance; BChl, bacteriochlorophyll; BPheo, bacteriopheophytine; Chl, chlorophyll; E_h, redox potential; EPR, electron paramagnetic resonance; *A*, optical absorbance; P, P-798, primary electron donor; P-700, Photosystem I primary electron donor; Pheo, pheophytine.

Correspondence: M.R. Fischer, Department of Biophysics, Huygens Laboratory of the State University, P.O. Box 9504, 2300 RA Leiden, The Netherlands.

0005-2728/90/$03.50 © 1990 Elsevier Science Publishers B.V. (Biomedical Division)

mediary electron acceptor in *Prosthecochloris aestuarii* [5], and suggests that this intermediary acceptor is a BChl *c*-like pigment. From EPR measurements it was inferred that a quinone acts as secondary acceptor [11], but after a 15 ns laser flash no light-induced changes can be attributed to the reduction of a quinone [12]. Another electron acceptor observed with EPR is an iron-sulphur cluster [7,11]; this has been confirmed by optical measurements [12]. Similar to Photosystem I, triplet signals have been difficult to detect. Up to now there has been only one report on the optical observation of such a signal [12].

The existing ambiguities in the structure of the electron transport chain of *H. chlorum* were the incentive to examine further the electron transfer mechanism by low-temperature EPR measurements under a variety of reducing conditions. Complex EPR signals in the $g = 2.00$ region were observed. Spectral simulations have been performed to identify the radicals responsible for these signals. Good agreement with the experimental results was obtained when it was assumed that the signals result from a convolution of EPR signals of the primary donor, a monomeric bacteriochlorophyll as first and a quinone as second acceptor. Furthermore, a triplet EPR signal has been found, which was interpreted to be a superposition of the EPR lines of an antenna- and a reaction centre triplet. Finally a split-line signal strikingly similar to that found in Photosystem II was observed [13].

Materials and Methods

H. chlorum was grown anaerobically in the light for 6 days in medium 112 of the American Type Culture Collection [1] containing in addition 2.5 mM sodium ascorbate. Cells were harvested and washed by centrifugation at $13000 \times g$ in a buffer (pH 8.5) containing 10 mM Tris, 10 mM sodium ascorbate and 2 mM dithiothreitol. Membrane fragments were prepared by sonication followed by centrifugation at $20000 \times g$ to remove unbroken cells and large fragments. They were then concentrated by ultracentrifugation at $265000 \times g$ on a 40% (w/v) sucrose layer.

In the presence of light, the extremely oxygen-sensitive BChl *g* absorbing at 788 nm is rapidly converted into a species absorbing at 670 nm [2,8,14]. Therefore all solutions used were thoroughly purged with nitrogen gas and further handling was done in the dark. The concentration of the degradation product was measured by the absorption ratio, A_{670}/A_{788}, which was usually smaller than 0.28.

Samples were prepared from fresh membrane fragments, which were diluted to an optical absorbance of 70 cm^{-1} with the buffer mentioned above to which 0.1 M glycine buffer (pH 10) was added, poising the sample at approx. pH 9.8. In addition, every sample contained 1.8% of 1 M glucose, and 0.9% of catalase and glucose-oxidase to keep it anaerobic. In a last step the redox chemicals were added, as will be described in the Results section.

No glycerol was added, since the samples contained enough viscous material to keep them from cracking during cooling slowly to liquid nitrogen temperatures in a flow cryostat. Samples were stored in 4 mm quartz EPR-tubes at 77 K, since storage of the fragments at 253 K deteriorated their activity.

X-band EPR measurements were performed on a Varian E9 spectrometer equipped with an Oxford Instruments helium-flow cryostat, using 100 kHz field modulation. *g* values were calibrated with DPPH (diphenylpicrylhydrazyl, $g = 2.0037$). Error limits of *g* and the peak-to-peak linewidth ΔB are 0.0002 and 0.05 mT, respectively, unless otherwise specified.

Illumination of the samples both during cooling to liquid nitrogen temperatures and at liquid helium temperatures was done with a 1000 W Aldis projection lamp, filtered through 5 cm of water to reduce the heating of the sample. Residual heating of the sample during illumination at 5 K was calibrated in the following way. The double integral of the EPR signal at $g = 2.00$ of a sample ($A = 70$ cm^{-1}, i.e., about 0.7 mM BChl for an extinction coefficient of chlorophylls of approx. 100 $cm^{-1} \cdot mM^{-1}$, or about 10 μM reaction centre concentration if one assumes approx. 1 reaction centre per 65 bacteriochlorophylls [15]) in which the primary donor P was fully oxidized by illumination during freezing to 77 K in the presence of 10 mM potassium ferricyanide (see Results), as measured in the dark at 5 K, was compared to the double integral of the signal obtained during illumination at 5 K. To check that P was indeed fully oxidized, 10 mM potassium ferricyanide was added to a sample with low optical absorbance ($A = 10$ cm^{-1}) that was then illuminated with a low-intensity lamp. No additional optical bleaching due to newly formed P^+ could be observed with laser flashes at room temperature. In view of the large excess of potassium ferricyanide in both the EPR and the optical sample, this conclusion also holds for the EPR experiment. Thus, for a fully oxidized sample the two spectra and therefore the number of spins should be identical when observed at 5 K in the dark and under illumination, because there is no 5 K light-induced signal. The observed difference detected must then be due to a temperature-induced change in the Boltzmann population ratio. The observed decrease of 46% of the value of the double integral of the P^+ signal under illumination then can be accounted for by a rise in temperature of 2.4 K. The sample used for calibration of the temperature-induced rise in signal had the same optical absorbance as the samples used in the other experiments. All double integrals of EPR signals

obtained under illumination have been corrected for this temperature effect.

Results

All experiments described below have been repeatedly performed in samples made of membrane preparations of different batches of *H. chlorum*. The spectra and other results given below are representative examples.

The primary donor, P^+

Illumination at 5 K of a sample prepared as described in Materials and Methods without any extra additions generated irreversibly a gaussian EPR signal at $g = 2.0027$ having a linewidth of 1.05 mT. The same line was generated by illuminating a sample containing 10 mM potassium ferricyanide during freezing to 77 K and observing the EPR signal in the dark at 5 K (Fig. 1A). This EPR signal is attributed to the primary donor P^+; its g value and linewidth agree with the data of Prince et al. [7].

The microwave power dependence of the amplitude of this signal is depicted in Fig. 2, the solid line representing a fit of the dependence according to Rupp's expression [16]:

$$I(P) = k\sqrt{P}\,[1 + P/P_{1/2}]^{-b/2} \quad (1)$$

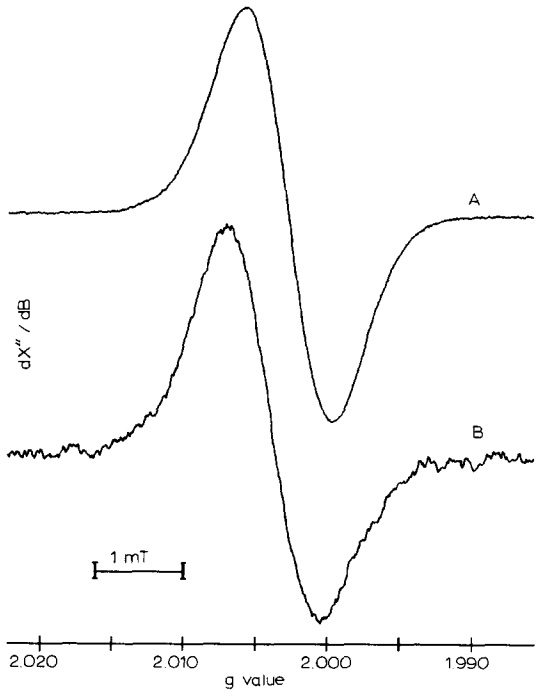

Fig. 1. (A) EPR spectrum of *H. chlorum* membrane fragments frozen under continuous illumination in the presence of 10 mM potassium ferricyanide and recorded at 5 K in the dark. Modulation amplitude, 0.2 mT; microwave power, 2 μW. (B) Sample FL, frozen under illumination in the presence of 10 mM potassium ferrocyanide and recorded at 5 K in the dark. Spectrometer settings as above.

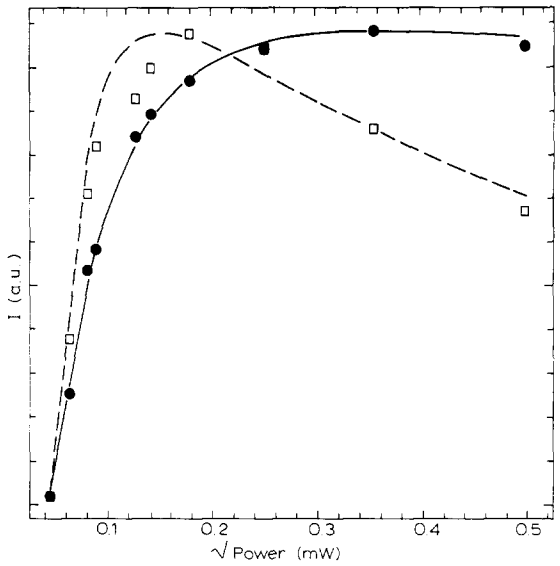

Fig. 2. The power dependence of the amplitude of the signal of the primary donor (●) and of the dark spectrum of sample FL (□). The solid and dashed lines are fits using Rupp's expression (Eqn. 1) [16] with $P_{1/2} = 9.5$ μW and 14 μW, and $b = 1.07$ and 1.4, respectively.

where I is the signal intensity, P the incident microwave power, $P_{1/2}$, the value of P at half-saturation, is 9.5 μW, $b = 1.07$ and k is a scaling constant. Measurements in the $g = 2.00$ region were always performed at a microwave power well below the value of $P_{1/2}$.

The acceptor complex

To produce different redox states, identical aliquots of *H. chlorum* membrane fragments were treated as follows:

(i) sample FL: frozen under continuous illumination in the presence of 10 mM potassium ferrocyanide;
(ii) sample DD: frozen in the dark in the presence of 30 mM sodium dithionite and 10 mM potassium ferrocyanide;
(iii) sample DL: sample DD thawed and refrozen under illumination.

Sample FL observed in the dark at 5 K yielded the iron-sulphur signal peaking at $g = 1.93$ described earlier [7,11], and in addition a narrow signal at $g = 2.0037$, linewidth 1.10 mT (Fig. 1B). The narrow signal was an asymmetric gaussian at 2.0 μW microwave power, and became more symmetric with increasing microwave power. The microwave power dependence of the amplitude of this signal is shown in Fig. 2, with the dashed line representing a fit with the half-saturation power $P_{1/2} = 14$ μW for $b = 1.4$. When this sample was thawed and refrozen in the dark, both the $g = 2.0037$ and the iron-sulphur signal disappeared; they reappeared when the sample was thawed and refrozen under illumination.

In order to describe the complex behaviour of the samples containing sodium dithionite not only the g values and the peak-to-peak linewidths were measured,

TABLE I

g values and peak-to-peak linewidths of the reduced acceptors

Sample [a]	g (± 0.0002)	ΔB [b] (mT) (± 0.05)	I [c] (a.u.) ($\pm 5\%$)	Fe-S (g) (± 0.005)	A [d] (a.u.) ($\pm 5\%$)
FL					
dark	2.0037	1.10		1.93	
DD					
dark before illumination [e]	2.0040 ± 0.0013	1.3 ± 0.2	215	1.93	99
during illumination	2.0028	1.08	2120	1.93	143
dark after illumination	2.0034	1.23	1050	1.93	101
DL					
dark before illumination	2.0037	1.36	920	1.93	248
during illumination	2.0037	1.23	1630	1.94	348
dark after illumination	2.0037	1.32	1380	1.93	267

[a] Samples were prepared as described in the text.
[b] ΔB, peak-to-peak width.
[c] I, double integral of the $g = 2.00$ signal.
[d] A, amplitude of the iron-sulphur first-derivative EPR-signal measured at $g = 1.93$.
[e] Increased error limits due to low signal intensity (Fig. 3A(a)).

but also the signal's double integral was determined, which is proportional to the number of spins. The value of the double integral was corrected for temperature effects as described in Materials and Methods (Table I).

Sample DD, frozen in the dark, exhibited only a very small signal when observed at 5 K in the dark before any illumination had taken place (Fig. 3A(a)). Due to this low intensity its g value and linewidth could only be determined with relatively large limits of error: $g = 2.0040 \pm 0.0013$, $\Delta B = 1.3 \pm 0.2$ mT. As soon as the light was switched on, a large asymmetric signal emerged with a g value of 2.0028 and $\Delta B = 1.08$ mT (Fig. 3A(b)). When the light was turned off again, an asymmetric signal at $g = 2.0034$ and $\Delta B = 1.23$ mT remained (Fig. 3A(c)). The intensity of this signal was approx. 60% of the (corrected) intensity of the light-induced signal.

Freezing the DD sample under illumination resulted in sample DL. Now a large signal at $g = 2.0037$, $\Delta B = 1.32$ mT was detected in the dark before any low-temperature illumination had taken place (Fig. 3B(a)). During illumination at 5 K the signal retained its g value, but became less wide, 1.23 mT, and its intensity almost doubled (Fig. 3B(b)). Switching the light off diminished its intensity to 85% and increased ΔB to 1.32 mT (Fig. 3B(c)).

In addition to the lines in the $g = 2.00$ region described above the iron-sulphur spectrum was observed. The signal of the iron-sulphur cluster of sample FL was identical to that of samples DD and DL observed in the dark. Close examination revealed that the spectra of sample DL detected in the dark and in the light were not identical: the g value of the light-induced spectrum (Fig. 4b) is slightly larger than that of the spectra

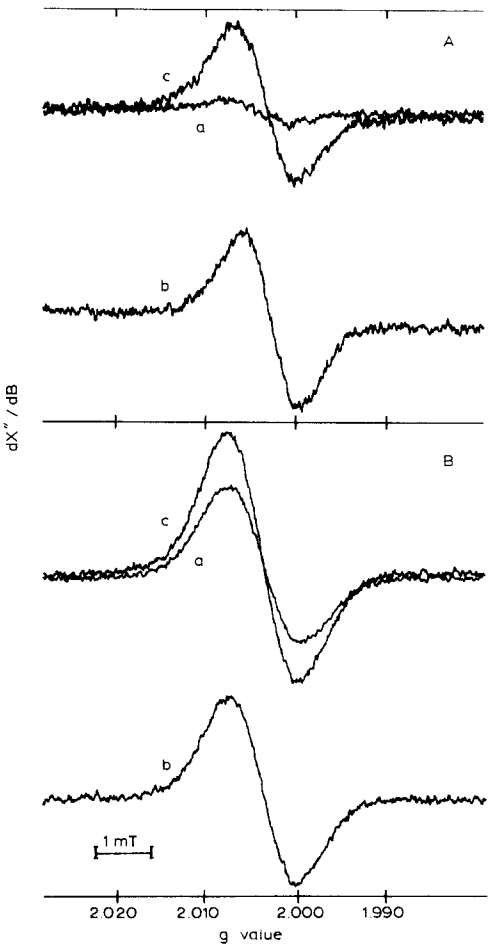

Fig. 3. (A) Spectra of sample DD in the $g = 2.0$ region, prepared as described in the text and recorded at 8 K before (a), during (b) and after illumination (c) at 8 K. Spectrometer settings as in Fig. 1A. (B) Same as above for sample DL.

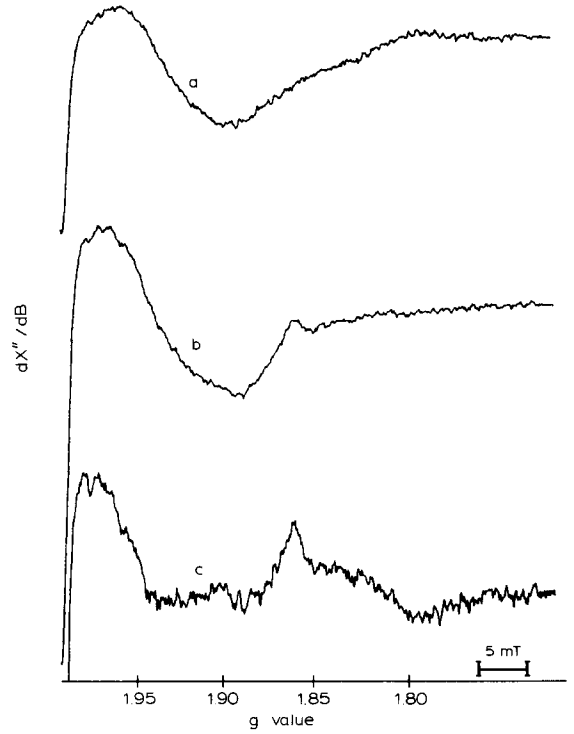

Fig. 4. The signal of the iron-sulphur cluster in sample DL recorded at 8 K before (a) and during (b) illumination, and the difference spectrum (c). Microwave power, 1 mW; modulation amplitude, 1.25 mT.

observed in the dark (Fig. 4a; see Table I). This difference is small, but it was consistently observed. The light-induced iron-sulphur signal is more clearly seen after subtraction of the dark signal from the light signal (Fig. 4c). I suggest that it results from an iron-sulphur cluster different from that seen in both samples in the dark.

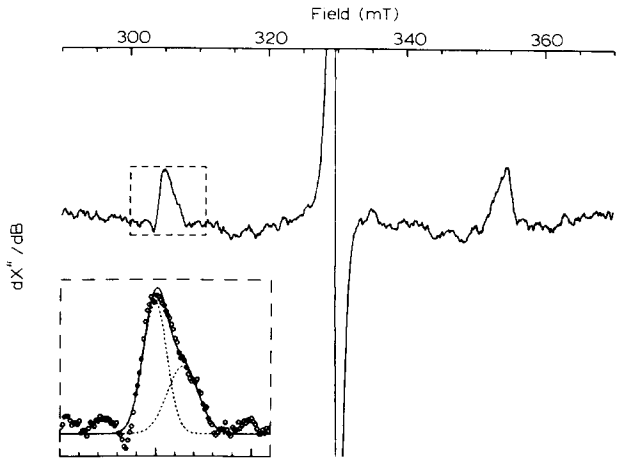

Fig. 5. Light-minus-dark difference spectrum of a sample reduced with 30 mM sodium dithionite frozen in the dark. Inset: enlargement of the low field triplet peak (points) with a simulation (drawn line) using two gaussian lines with midfield, peak-to-peak width and amplitude 304.95 mT, 1.47 mT, 212.3 and 306.42 mT, 1.90 mT and 109.7, respectively. Temperature, 8 K; microwave power, 0.2 mW; modulation amplitude, 1.25 mT. The spectrum is the average of 16 scans.

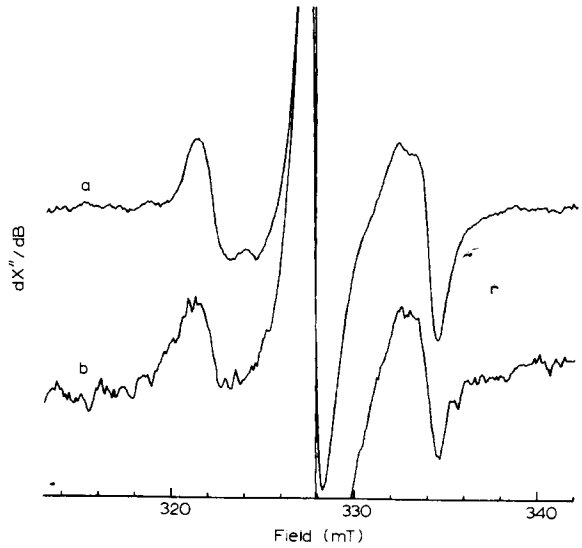

Fig. 6. (a) The split-line difference spectrum measured at 5 K in the dark before illumination and during illumination. Sample reduced with 0.5 M sodium ascorbate and frozen in the dark. (b) Same for Tris-washed Photosystem II chloroplast particles. Microwave power, 1 mW; modulation amplitude, 1.25 mT.

The triplet

A light-induced triplet spectrum was detected when an anaerobic sample was reduced with 30 mM sodium dithionite in the dark (Fig. 5). It consists of one pair of peaks centered at $g = 2.00$ and spaced by 51.6 mT. Each of the peaks consists of two superimposed gaussian lines, both of which are absorptive (low field) or emissive (high field) (Fig. 5, inset).

The split-line signal

When 0.5 M sodium ascorbate is added to an anaerobic, freshly prepared sample, an irreversible split-line signal appears when illuminating at 5 K (Fig. 6). The resonances are centered around $g = 2.0$ at $g = 2.043$ and $g = 1.963$, split by approx. 12.0 mT and show almost no power dependence. With the appearance of the doublet, a peak at $g = 2.025$ that was present in almost every sample diminished strongly in intensity.

Discussion

The primary donor

The primary donor signal is a near-perfect symmetric gaussian line (Fig. 1A), with a peak-to-peak width of 1.05 mT at 5 K, in good agreement with the data of the primary donor signal of Prince et al. [7]. Brok et al. [11] found a considerably higher peak-to-peak width, $\Delta B = 1.30$ mT at 8 K. Since both chemically-oxidized samples and samples without additions yielded the same peak-to-peak width, it is highly unlikely that variations in the ambient redox potential can give rise to this discrepancy. Probably, the difference is due to the use by

TABLE II

g values and widths of various chlorophyll and pheophytin anions and cations

	Anion/ cation	g value	ΔB (mT)	Solvent	Ref.
Chl *a*	+	2.0025	0.9	CH_2Cl_2	19
	+	2.0026	0.9	CH_2Cl_2	20
	–	2.0029	1.21–1.35	DMF	20, 21, 22
Pheo *a*	–	2.0030	1.22–1.31	DMF	20, 21, 22
BChl *a*	+	2.0025	1.32	CH_2Cl_2	23
	+	2.0025	1.28	$CHCl_3$	23
	+	2.0025	1.3	CH_2Cl_2/CH_3OH	24
	–	2.0028	1.27	THF	25
	–	2.0028	1.0	butyronitrile	26
BPheo *a*	+	2.0026	1.44	CH_2Cl_2	23
	+	2.0026	1.40	$CHCl_3$	23
	–	2.0032	1.22–1.30	C_5H_5N/H_2O	24
	–	2.0033	1.22–1.30	CH_2Cl_2	25
	–	2.0030	1.30	CH_2Cl_2	27
BChl *b*	+	2.0025	1.39	CH_2Cl_2/CH_3OH	28
	+	2.0025	1.40	CH_2Cl_2/CH_3OH	24
	+	2.0027	0.84	ethanol	29
	–	2.0033	1.28–1.30	MeTHF	28, 30
BPheo *b*	–	2.0033	1.22–1.30	CH_2Cl_2	28
	–	2.0033	1.22–1.30	C_5H_5N/H_2O	24, 30
BChl *c*	–	2.0032–34	1.18–1.27	in vivo	31
BPheo *c*	–	2.0032–34	1.18–1.27	in vivo	31
BChl *g*	+	2.0025	0.95	in vivo	7
	+	2.0025	1.20	in vivo	11
	+	2.0027	1.05	in vivo	this work
BPheo *g*	+	2.0025	0.95	tetranitromethane	32

Brok et al. [11] of less well-defined membrane fragments in samples that were not freshly prepared.

The acceptor complex

The samples containing 30 mM sodium dithionite yielded spectra of lower intensity when they were frozen in the dark than when they were frozen under illumination. This indicates that even at a redox potential as low as $E_h \leqslant -0.530$ V (30 mM sodium dithionite, pH 9.8) it is not possible to chemically reduce all acceptors. Apparently, the reduced form of these acceptors can be photo-accumulated by combining illumination and chemical reduction.

To test whether the incomplete reduction of the acceptors by sodium dithionite was due to inadequate accessibility to the reductant, samples to which 10 mM potassium ferrocyanide was added, were compared to sodium-dithionite-reduced ones. Potassium ferrocyanide has not only a different redox potential, but also a different hydrophobicity and a different size compared with sodium dithionite. This presumably would give rise to a different accessibility of the acceptors for these reductants. However, no differences were detected.

The variety of observed g values and peak-to-peak widths listed in Table I cannot be explained with a sequence consisting of only one acceptor in addition to the iron-sulphur cluster(s), such as described for the green sulphur bacteria. Additional support for the notion that there are two radical acceptors is given by a microwave power dependence study of samples DD and DL before illumination at 5 K (data not shown). In these cases one can assume that only the complex $(A_0A_1)^-$ is present. For sample DD, the signal-to-noise ratio does not permit any conclusions to be drawn concerning the g values and linewidths at the various powers. For sample DL the lineshape became more symmetric with increasing power, while the g value did not change. This behaviour is similar to that described above for the power dependence of sample FL. This suggests that there is more than one acceptor present. An alternative interpretation, i.e., molecular motion of a molecule with a strong hyperfine anisotropy [17] is less likely, because of the low temperature of measurement and the absence of large, anisotropic hyperfine couplings in the radicals under consideration. Photosystems in which more than one acceptor besides the iron-

sulphur clusters are present, such as Photosystem I, appear to have an acceptor chain consisting of a (bacterio)chlorophyll as first acceptor, A_0, followed by a quinone, A_1 (for a review see Ref. 18).

Brok et al. [11] found indications for a quinone acceptor in *H. chlorum* so that it was an obvious choice to attempt to explain the observed complex behaviour by using Photosystem I as the guiding principle for *H. chlorum*. Thus, it was assumed that there are two $g = 2.00$ acceptors, one chlorophyll-like, A_0, and one quinone-like, A_1. The suggestion from optical measurements that A_0 is a BChl *c*-type molecule [5] is based on an absorption difference band at 670 nm. The presence of BChl *c* in the reaction centre of *H. chlorum*, however, has not been assessed by chemical analysis or other means. For the simulation a broader variety of chlorophyll-like A_0 has therefore been examined, viz. a BChl *g* mono- or dimer, a BChl *c* monomer, or a bacteriopheophytin (BPheo) *g* or *c* monomer. Note that the BChl *c* and BPheo *c* anions are dihydroporphyrins, whose EPR signals will have a width similar to that of Chl a^- and Pheo a^-, viz. approx. 1.21–1.35 mT and 1.22–1.31 mT, respectively (see Table II).

The acceptor complex A_0A_1 can be singly or doubly reduced. In the latter case, there may be an exchange interaction, $J(A_0^-A_1^-)$, which was taken into account using the formalism of Schepler et al. [33]. Note that the lineshape of the EPR spectrum of exchange coupled radicals is independent of the sign of $J(A_0^-A_1^-)$.

For the simulations, the following assumptions were made:

(i) The oxidized primary donor P^+ is a BChl *g* dimer cation radical with $g = 2.0026$ and $\Delta B = 1.05$ mT.

(ii) The reduced first acceptor, A_0^-, is either a BChl *g* monomer or dimer anion radical with $g = 2.0026$ and $\Delta B = 1.30$ mT or 1.00 mT, respectively, or it is the anion radical of a BPheo *g* or *c* monomer with $\Delta B = 1.30$ mT or of a BChl *c* monomer with $\Delta B = 1.00$ mT, all with $g = 2.0033$ (see Table II).

(iii) The reduced second acceptor anion radical, A_1^0, is a quinone having a *g* value between 2.0040 and 2.0060 and a peak-to-peak width of 0.90 mT or 1.00 mT.

(iv) During low-temperature illumination of the samples the iron-sulphur cluster(s) is (are) reduced reversibly. There are reversible and non-reversible light-induced changes in the $g = 2.00$ region. The amplitude *A* of the iron-sulphur centre in the dark is the same before and after 5 K illumination in both samples DD and DL (see Table I). The reversible changes in the $g = 2.00$ region are therefore correlated with the reversible changes of the iron-sulphur signal. The *g* value and linewidth of the DD sample under illumination indicate that P^+ strongly predominates over $(A_0A_1)^-$. About one-fourth of the signal in the light is due to irreversibly induced $(A_0A_1)^-$ (sample DD after illumination). Any significant amount of reversibly induced $(A_0A_1)^-$ would push the *g* value and linewidth of the $g = 2.00$ signal in the light well beyond the measured values. It is therefore assumed that the first or second acceptor A_0 and A_1 is reduced irreversibly (Table I).

(v) In singly reduced reaction centres, state $(A_0A_1)^-$, one may have a distribution of the states $A_0^-A_1$ and $A_0A_1^-$, either because of a redox equilibrium between these states, or because of heterogeneity in the reaction centre ensemble. The ratio of the concentrations of the states $A_0^-A_1$ and $A_0A_1^-$, expressed in the parameter $m = I_{A_0}/I_{A_1}$ (see below), is not known. It is assumed that *m* does not depend on the redox conditions used. For the simulations *m* is varied between 0 and 4.

(vi) Doubly-reduced reaction centres are present in a fraction, *p*, of the reaction centres; *p* may vary between the various samples; in this fraction, *p* A_0^- and A_1^- are exchange coupled.

(vii) Since the actual molecular identity and hence the principal *g* values of the quinone type acceptor are not known, the EPR lines of all individual components are represented by symmetric gaussians with isotropic *g* values. For X-band this assumption does not greatly influence the lineshape of the reduced quinone type acceptor.

It was not possible to determine the separate contributions of P^+, A_0^- and A_1^- to the $g = 2.00$ signal directly from the experiments. Therefore the double integrals of the $g = 2.00$ signals were taken as a direct measure of the total amount of all radicals. To calculate the individual contributions the following procedure was adopted, using the assumptions described above.

Let the amount of oxidized primary donor, the first and second reduced acceptor A_0^- and A_1^- be represented by I_P, I_{A_0} and I_{A_1}, respectively. Then it is possible to write down equations for the number of spins of the above-mentioned radicals taking part in the six different redox states. These equations of course do not describe the absolute number of spins, but their relative amounts. Note that the calculations are performed for redox states of the same sample, under identical measuring conditions.

In sample DD one expects that before illumination there will be no P^+ present, so in this case the equations are (Table I):

$$I_P(0) = 0$$

$$I_{A_0}(0) + I_{A_1}(0) = 215 \qquad (2)$$

During illumination at 5 K there will be a certain amount of light-induced P^+ associated with the reduced iron-sulphur cluster, $I_P(FeS^-)$, and in addition an

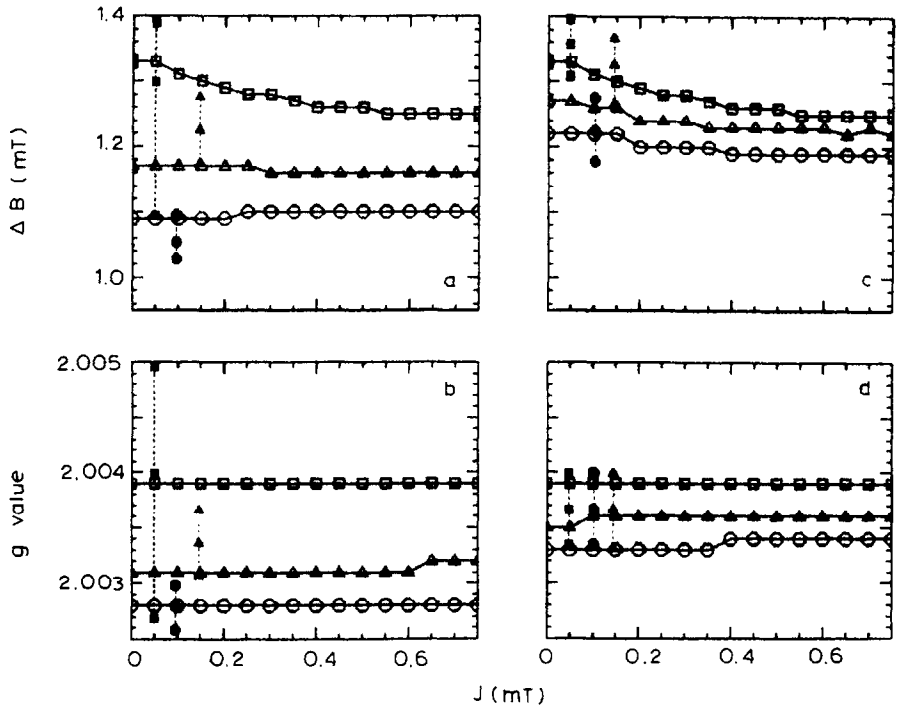

Fig. 7. Simulation of (a, c) the peak-to-peak width and (b, d) the g value of sample DD and sample DL, respectively, for $m = 1$, $p = 0.2$ (see text) and varying exchange coupling $J(A_0^- A_1^-)$. □, before; ○, during; and △, after low temperature illumination at 5 K. $\Delta B(A_0^-) = 1.30$ mT, $g(A_0^-) = 2.0026$, $\Delta B(A_1^-) = 1.00$ mT, $g(A_1^-) = 2.0054$.

amount associated with the light-induced reduced acceptors A_0^- and A_1^-, $I_P(A_0^- + A_1^-)$:

$$I_P(FeS^-) + I_P(A_0^- + A_1^-) + I_{A_0} + I_{A_0}(0) + I_{A_1} + I_{A_1}(0) = 2120. \quad (3)$$

Since the iron-sulphur signal is completely reversible (assumption (iv)), only the amount of P^+ associated with the irreversibly-reduced A_0^- and A_1^- will remain after switching off the light:

$$I_P(A_0^- + A_1^-) + I_{A_0} + I_{A_0}(0) + I_{A_1} + I_{A_1}(0) = 1050. \quad (4)$$

Combining Eqns. 2 and 4 yields the amount of irreversibly light-induced radicals, and because the sum of the amount of light-induced reduced first and second

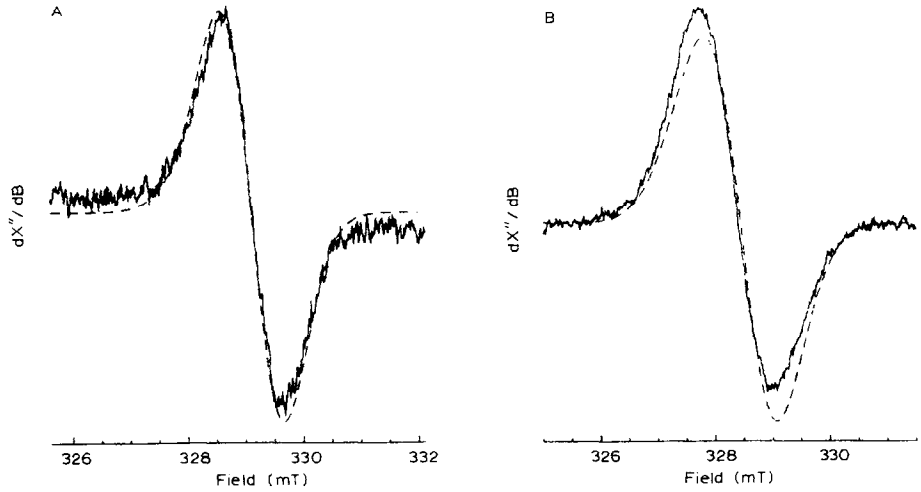

Fig. 8. (A) Comparison of experimental (———) and simulated (- - - - - -) spectra for sample DD during illumination at 5 K. Simulation parameters: $m = 1$, $p = 0.2$, $J(A_0^- A_1^-) = 0.1$ mT. $\Delta B(A_0^-)$, $g(A_0^-)$ $\Delta B(A_1^-)$ and $g(A_1^-)$ as in Fig. 7. (B) Same as (A) for sample DL after illumination at 5 K.

acceptor radicals is equal to the amount of light-induced oxidized primary donor, one determines the amount of P^+ as $I_P(A_0^- + A_1^-) = 417$. It is of course not possible to determine the relative concentration I_{A_0}/I_{A_1}. For sample DL one can find a similar set of equations, which yields $I'_P(A_0^- + A_1^-) = 230$.

One can now rewrite Eqns. 2 to 4 in terms of I_{A_1} by using the relative concentration $m = I_{A_0}/I_{A_1}$ as a parameter and assuming that m remains constant under all the experimental conditions (assumption (v)). Simulations of the $g = 2.00$ signals were carried out for all different combinations of the acceptors as described in assumptions (i) to (iii). Eqns. 2 and 4 were rewritten in I_{A_1} and m, and the value m varied from 0 to 4. In addition, for all samples the fraction p was varied between 0 and 1, and $J(A_0^- A_1^-)$ between 0 and 0.75 mT.

The stick spectrum calculated for the different combinations of the reduced acceptors A_0^- and A_1^- (assumptions (i) to (iii)) consists of seven sticks: one each for the signal of P^+, A_0^- and A_1^- in singly-reduced reaction centres and four due to the exchange interaction in doubly-reduced reaction centres. These sticks were then dressed with gaussians having the appropriate width. In selecting acceptable fits, the first selection criterion was the g value. For the set of spectra with the correct g value (within error limits ± 0.0003) the peak-to-peak widths were examined. Acceptable fits are found only for A_0^- having a g value of 2.0026 and a linewidth of 1.3 mT, while the A_1^- must have a g value close to 2.0054 and $\Delta B = 0.9$ to 1.0 mT. The former result implies that if A_0^- is a BChl *c*-type anion, it must have a molecular structure that is fairly different from that of Chl a^- to accommodate its much larger linewidth. For example, the β-protons of the saturated pyrrole could be somewhat twisted from the position they have in Chl *a* (see, for example, Ref. 28). On the other hand, if it is a BChl *g* monomer, the absorption difference band at 670 nm is not easily explained. The present results rule out a BChl *g* monomer. The *g* value and linewidth of A_1^- fall well within the range expected for a quinone-type molecule and corroborate the results of Brok et al. [11].

From a coarse-grid search, fitting *all* six spectra simultaneously (e.g., Fig. 7), the following values for m, p and the exchange interaction $J(A_0^- A_1^-)$ were obtained: $m = 1.0 \pm 0.2$, $p = 0$ to 0.3 and $J(A_0^- A_1^-) \leqslant 0.2$ mT. In Fig. 8, two simulated spectra, for samples DD and DL, give an impression of the fits. The overall agreement between experimental and simulated spectra is satisfying, especially in view of the fact that the line *shape* was not used as a selection criterion. The spectra of Fig. 8 bracket the range of goodness of fit for the fit parameters used, the simulation of Fig. 8A giving the best and that of Fig. 8B the worst agreement with the experiment. Simulations for the other four experimental spectra lie inbetween (not shown). The spectra of sample DD were typically better fitted than those of sample DL. This is probably due to the larger relative amount of acceptor radicals in the latter sample, accentuating the somewhat anisotropic quinone signal, whose anisotropy was not taken into account in the simulation (assumption (vii)). For $p = 0$ the fits are less good, but still within the error limits, so that it cannot be excluded that none of the reaction centres is doubly reduced. The finding that m is approx. 1 implies that if the distribution of the negative charge over A_0 and A_1 is due to a redox equilibrium, then the redox midpoint potentials should be similar. This would be surprising in a linear electron transport chain. Teleologically it is unlikely that a reaction centre BChl molecule not engaged in normal electron transport is in redox equilibrium with the quinone acceptor. Moreover, the redox midpoint potentials of BChl *c* and BPheo *c* are -1.03 V and -0.79 V in CH_2Cl_2, respectively [31], whereas the predicted redox potential of BChl *g* is similar to that of BChl *b* [34], which is -0.70 V in DMF/ClO_4^- and similarly for BPheo *g* and BPheo *b* (-0.56 V [30]), i.e., all are considerably lower than those of quinones in other bacterial reaction centres, which are in the range of -0.020 V to -0.160 V (for a review see Ref. 35). (Note, however, that in Photosystem I a quinone may function at a redox-potential as low as -1.040 V [36].) It is therefore tentatively concluded that in the present membrane preparations of *H. chlorum* the reaction centres are heterogeneous in the sense that about half of them lack the quinone acceptor. In those reaction centres, under the experimental conditions of this work, the back-reaction between photo-produced P^+ and A_0^- is apparently inhibited. This contrasts with the situation in Photosystem I, where at low temperatures under appropriate redox conditions P-700 is reversibly photo-oxidized [37]. The fact that there are probably two populations does not necessarily imply that this must be a preparation artefact, because then this would depend on the different batches, which is not the case. If indeed $p \neq 0$ in, for example, the DL sample, then the simulations require that the value of $J(A_0^- A_1^-)$ is quite low, $J(A_0^- A_1^-) \leqslant 0.2$ mT. This is much too small to shift an acceptor *g* value to 2.0017 as proposed for Photosystem I [38]. In that case, either $J(A_0^- A_1^-)$ in Photosystem I is much larger than in *H. chlorum*, or the plant and bacterial reaction centres differ in their proclivity to double reduction. Note, however, that also the higher value of $g = 2.0024$ has been suggested for A_0^- in Photosystem I [39], which value is more compatible with a small $J(A_0^- A_1^-)$. While for Photosystem I p is close to unity [38], p of *H. chlorum* might be zero, but then of course $J(A_0^- A_1^-)$ cannot be extracted from the present results.

A striking result is the complete reversibility of the large light-induced $g = 1.93$ iron-sulphur signal at 5 K,

whereas the signals of the $g = 2.00$ acceptors are irreversibly induced by illumination at low temperatures. In current thinking and by analogy to Photosystem I the iron-sulphur clusters are the 'last' acceptors of the electron transfer chain, after the $g = 2.00$ acceptors. It is therefore remarkable that the iron-sulphur clusters are reversibly reduced instead of the $g = 2.00$ signals. It is unlikely that the iron-sulphur is placed before the other acceptors, because of its relatively high redox potential [7]. One has therefore to assume that at 5 K and under the condition of photo-accumulation, in part of the reaction centre population the iron-sulphur cluster is reduced instead of the BChl/quinone acceptor complex. It is clear that further experiments with, for example, Q-band EPR are needed to shed more light on this puzzling effect.

The triplet signal

To augment the present results, the triplet signal in *H. chlorum* has also been studied by ADMR spectroscopy (Lous, E.J. and Hoff, A.J., unpublished experiments). With this technique two triplets were detected with zero-field splitting parameters $|D| = (240$ and 226 $(\pm 10)) \cdot 10^{-4}$ cm^{-1}, and $|E| = (88$ and 74 $(\pm 10)) \cdot 10^{-4}$ cm^{-1}, respectively. On the basis of their triplet-minus-singlet absorbance difference spectra these triplets were attributed to the reaction centre triplet and a triplet state of an antenna pigment, respectively. On close inspection of the EPR triplet signal one sees that each of the two peaks consists of two gaussian lines (Fig. 5, inset). The centre fields of the gaussian lines are 1.47 mT apart. If one assumes that the two gaussian lines represent the z- and x-triplet peak of one species, then $|D| = 241 \cdot 10^{-4}$ cm^{-1} and $|E| = 72 \cdot 10^{-4}$ cm^{-1}. If the two lines are attributed to two different triplet species, then $|D_1| = 241 \cdot 10^{-4}$ cm^{-1} and $|D_2| = 227 \cdot 10^{-4}$ cm^{-1}, and the $|E|$ values cannot be determined. The latter values of $|D|$ are very close to those found in the ADMR experiments. Therefore the first triplet, characterized by $|D_1|$ and $|E_1|$, is assigned to the reaction centre triplet ^{3}P, and the smaller peaks to an antenna triplet. The latter may be located on a BPheo g molecule, for which $|D| = 225 \cdot 10^{-4}$ cm^{-1} and reportedly $|E| = 15 \cdot 10^{-4}$ cm^{-1} [32]. The relatively high intensity of the antenna z-peak overlaps with the x-peak of the reaction centre triplet, rendering this unobservable. Since the amplitudes of both triplet signals are rather small, the much less intense y-peaks could not be detected. These peaks are spaced ($|D| - 3|E|$) around $g = 2.00$, but they are overlapped by the $g = 2.00$ signal and cannot be detected. This is the case both for one or two triplet species. Of course the spacing ($|D| - 3|E|$) cannot be smaller than 0. For the reaction centre triplet, a very small spacing lies within the limits of error of the values of $|D|$ and $|E|$ determined by ADMR, i.e., $|E|$ is probably close to $|D|/3$. Note, that the sign of the z-peaks of the reaction centre triplet (the outermost peaks) is compatible with the so-called $S - T_0$ spin mixing mechanism (for a review see Ref. 40), and that those of the antenna triplet have the same sign as found for the z-peaks in the Bpheo g triplet [32].

The split-line signal

The split-line spectrum found at 5 K shows a splitting of 12.0 mT. A similar split-line spectrum has been found by Rutherford and Thurnauer in Tris-washed Photosystem II particles [13]. In Fig. 6 the split-line spectrum of *H. chlorum* is compared with the one recorded at 5 K for Photosystem II particles prepared as in Ref. 13. It is seen that the two spectra are remarkably similar. In Photosystem II preparations the splitting varied between 10.0 and 8.5 mT in the range of 5 to 80 K, and was attributed [13] to a dipolar magnetic interaction between the secondary donor radical, D^+, a tyrosine [41,42,43], and the intermediary acceptor, I^-, a pheophytin [44].

The similarity between the split-line spectra of *H. chlorum* and Photosystem II suggests that under the conditions of the observation an oxidized secondary donor has a magnetic interaction with one of the reduced acceptors. This secondary donor might be a cytochrome c-type donor, which is known to be present in *H. chlorum* [7,8], but these donors generally have high-field g values that are above $g = 2.3$. A search for light-induced changes in the EPR spectrum at g values higher than 2.05 was unsuccessful. Alternatively, the secondary donor may be a blue copper protein, such as plastocyanin, which is the secondary donor in plant photosystems with $g_\perp = 2.05$ [45]. In *C. aurantiacus*, a green filamentous bacterium, such a protein, called auracyanin, has been detected [46], and a possible explanation might thus be that the $g = 2.025$ signal, which is present prior to reduction, is a cyanin signal. When the split-line signal appears, the cyanin signal at $g = 2.025$ diminishes due to the magnetic interaction between the cyanin and an acceptor. Further experiments will have to be performed to determine whether such a cyanin is present in *H. chlorum*.

Acknowledgements

I thank Drs. J. Amesz, H.J. van Gorkom and A.J. Hoff for advice and stimulating discussions, and the latter especially for carefully reading the manuscript. I am indebted to Mr. F. Vergeldt for assistance with some of the experiments. The ADMR results were kindly provided by Drs. E.J. Lous and A.J. Hoff. I am obliged to Mr. A.H.M. de Wit and Ms. M.L. van der Erf for culturing the bacteria. The investigation was supported by the Netherlands Foundation for Chemical Research (SON) with financial aid from the Netherlands Organization for Scientific Research (NWO).

References

1 Gest, H. and Favinger, J.L. (1983) Arch. Microbiol. 136, 11–16.
2 Brockmann, Jr., H. and Lipinski, A. (1983) Arch. Microbiol. 136, 17–19.
3 Blankenship, R.E. (1984) Photochem. Photobiol. 40, 801–806.
4 Woese, C.R., Debrunner-Vossbrinck, B.A., Oyaizu, H., Stackebrandt, E. and Ludwig, W. (1985) Science 229, 762–765.
5 Nuijs, A.M., Van Dorssen, R.J., Duysens, L.N.M., Amesz, J. (1985) Proc. Natl. Acad. Sci. USA 82, 6865–6868.
6 Van Dorssen, R.J., Vasmel, H. and Amesz, J. (1985) Biochim. Biophys. Acta 809, 199–203.
7 Prince, R.C., Gest, H. and Blankenship, R.W. (1985) Biochim. Biophys. Acta 810, 377–384.
8 Fuller, R.C., Sprague, S.G., Gest, H. and Blankenship, R.E. (1985) FEBS Lett. 182, 345–349.
9 Fajer, J., Barkigia, K.M., Fujita, E., Goff, D.A., Hanson, L.K., Head, J.D., Horning, T., Smith, K.M. and Zerner, M.C. (1984) in Proceedings of the Feldafing Workshop on Antennas and Reaction Centers of Photosynthetic Bacteria (Michel-Beyerle, M.E., ed.), pp. 324–338, Springer, Berlin.
10 Hanson, L.K. and Fajer, J. (1985) Biophys. J. 47a, 422a.
11 Brok, M., Vasmel, H., Horikx, J.T.G. and Hoff, A.J. (1986) FEBS Lett. 194, 322–326.
12 Smit, H.W.J., Amesz, J. and Van der Hoeven, M.F.R. (1987) Biochim. Biophys. Acta 893, 232–240.
13 Rutherford, A.W. and Thurnauer, M.C. (1982) Proc. Natl. Acad. Sci. USA 79, 7283–7287.
14 Beer-Romero, P., Favinger, J.L. and Gest, H. (1988) FEMS Microbiol. Lett. 49, 451–454.
15 Vos, M.H., Klaassen, H.E. and Van Gorkom, H.J. (1989) Biochim. Biophys. Acta 973, 163–169.
16 Rupp, H., Rao, K.K., Hall, D. and Cammack, R. (1978) Biochim. Biophys. Acta 537, 255–269.
17 Hyde, J.S., Eriksson, L.E.G. and Ehrenberg, A. (1970) Biochim. Biophys. Acta. 222, 688–692.
18 Andréasson, L.-E. and Vånngård, T. (1988) Annu. Rev. Plant Physiol. Plant Mol. Biol. 39, 379–411.
19 Borg, D.C., Fajer, J., Felton, R.H. and Dolphin, J. (1970) Proc. Natl. Acad. Sci. USA 67, 813–820.
20 Fajer, J., Fujita, I., Davis, M.S., Forman, A., Hanson, L.K. and Smith, K.M. (1982) Adv. Chem. Ser. 201, 489–513.
21 Fujita, I., Davis, M.S. and Fajer, J. (1978) J. Am. Chem. Soc. 100, 6280–6282.
22 Fajer, J., Davis, M.S., Forman, A., Klimov, V.V., Dolan, E. and Ke, B. (1980) J. Am. Chem. Soc. 102, 7143–7145.
23 Fajer, J., Borg, D.C., Forman, A., Felton, R.H., Dolphin, D. and Vegh, L. (1974) Proc. Natl. Acad. Sci. USA 71, 994–998.
24 Fajer, J., Davis, M.S., Brune, D.C., Spaulding, L.D., Borg, D.C. and Forman, A. (1976) Brookhaven Symp. Biol. 28, 74–104.
25 Fajer, J., Forman, A., Davis, M.S., Spaulding, L.D., Brune, D.C. and Felton, R.H. (1977) J. Am. Chem. Soc. 99, 4134–4140.
26 Fajer, J., Borg, D.C., Forman, A., Dolphin, D. and Felton, R.H. (1973) J. Am. Chem. Soc. 95, 2739–2741.
27 Fajer, J., Brune, D.C., Davis, M.S., Forman, A. and Spaulding, L.D. (1975) Proc. Natl. Acad. Sci. USA 72, 4956–4960.
28 Davis, M.S., Forman, A., Hanson, L.K., Thornber, J.P. and Fajer, J. (1979) J. Phys. Chem. 83, 3325–3332.
29 Kim, V.A., Vosniak, V.M. and Estigneev, V.B. (1975) Biofizika 20, 208–212.
30 Fajer, J., Davis, M.S., Brune, D.C., Forman, A. and Thornber, J.P. (1978) J. Am. Chem. Soc. 100, 1918–1920.
31 Fajer, J., Fujita, I., Forman, A., Hanson, L.K., Craig, G.W., Goff, D.A., Kehres, L.A. and Smith, K.M. (1983) J. Am. Chem. Soc. 105, 3837–3843.
32 Michalski, T.J., Hunt, J.E., Bowman, M.K., Smith, U., Bardeen, K., Gest, H., Norris, J.R. and Katz, J.J. (1987) Proc. Natl. Acad. Sci. USA 84, 2570–2574.
33 Schepler, J.L., Dunham, W.R., Sands, R.H., Fee, J.A. and Abeles, R.H. (1975) Biochim. Biophys. Acta 397, 510–518.
34 Hanson, L.K. (1988) Photobiochem. Photobiol. 47, 903–921.
35 Prince, R.C. and Dutton, P.L. (1978) in The Photosynthetic Bacteria (Clayton, R.K. and Sistrom, W.R., eds.), pp. 439–453, Plenum, New York.
36 Nitsch, C., Braslavsky, S.E. and Schatz, G.H. (1988) Biochim. Biophys. Acta 934, 201–212.
37 Ke, B., Dolan, E., Sugahara, K., Hawkridge, F., Demeter, S. and Shaw, E.R. (1977) in Photosynthetic Organelles, special issue of Plant Cell Physiol., 187–199.
38 Gast, P., Swarthoff, T., Ebskamp, F.C.R. and Hoff, A.J. (1983) Biochim. Biophys. Acta 772, 163–175.
39 Bonnerjea, J. and Evans, M.C.W. (1982) FEBS Lett. 148, 313–316.
40 Hoff, A.J. (1984) Q. Rev. Biophys. 17, 153–282.
41 Barry, B.A. and Babcock, G.T. (1987) Proc. Natl. Acad. Sci. USA 84, 7099–7103.
42 Vermaas, W.J.F., Rutherford, A.W. and Hansson, O. (1988) Proc. Natl. Acad. Sci. USA 85, 8477–8481.
43 Debus, R.J., Barry, B.A., Babcock, G.T. and McIntosh, L. (1988) Biophys. J. 53, 270a.
44 Klimov, V.V., Klevanik, A.V., Shuvalov, V.A. and Krasnovsky, A.A. (1977) FEBS Lett. 82, 183–186.
45 Visser, J.W.M., Amesz, J. and Van Gelder, B.F. (1974) Biochim. Biophys. Acta 368, 235–246.
46 Trost, J.T., McManus, J.D., Freeman, J.C., Ramakrishna, B.L. and Blankenship, R.E. (1988) Biochemistry 27, 7858–7863.